Variability of Frontal Structure in the Southern Norwegian Sea

ZACHARIAH R. HALLOCK

Physical Oceanography Branch, Naval Ocean Research and Development Activity, NSTL Station, MS 39529

(Manuscript received 24 April 1984, in final form 15 March 1985)

ABSTRACT

A hydrographic survey (CTD) was conducted in the vicinity of the Iceland–Faeroe Island oceanic front (IFF) north of the Faeroe Islands during October 1980. It consisted of CTD transects on three horizontal scales ranging from kilometers to hundreds of kilometers.

Intense interleaving of different water masses is found in the IFF in the presence of horizontal current shear. Significant alongfront variability on scales of about 50 km is present, consistent with earlier findings. Estimates of cross-front heat flux of 5.16×10^4 W m^{-2} and salt flux of 1.58 g m^{-2} s^{-1} are greater than those found for the Antarctic Polar Front but are of the same order as eddy heat flux across the IFF found by Willebrand and Meincke. Evidence suggests that intrusive interleaving in the IFF on 50 m vertical scales is driven by double-diffusive convection.

1. Introduction

Background—The region including the oceanic polar front north of the Faeroe Islands in the southern Norwegian Sea has been the subject of several intensive studies. Most notable were the OVERFLOW '60 and '73 expeditions that described and quantified the outflow of Norwegian Sea deep water into the Atlantic Ocean. The extensive hydrographic results of Mueller (1979) and of Tait (1967) show a region rich in thermohaline variability on many scales in both the upper ocean and at depth due to the strong confluences of warm North Atlantic water and cold water of Arctic origin. Complex current interactions, particularly near the surface, make the area very interesting to study, yet difficult to describe. An adaptation of the surface current chart of Helland-Hansen and Nansen (1909) is presented in Fig. 1. The positions of the Jan Mayen, the Iceland-Faeroe Island, and the Norwegian Current fronts are indicated.

One of the principal findings of OVERFLOW '60 was that thermohaline variability shallower than 400 m was quite complex and changed significantly on weekly time scales. In particular, eddylike features were noted over the Iceland–Faeroe Ridge (IFR), which had horizontal scales of about 50 km. Temporal and spatial variability was less intense below 400 m, the nominal depth of the IFR. The hydrography of OVERFLOW '73 was less synoptic than that of OVERFLOW '60 and included extensive sections along and across the IFR. The results included quantifying water mass modification, identifying overspill features near the bottom, and describing mid-depth outflows and recirculation around the Faeroe Islands (Dooley and Meincke, 1981). In their analysis of current meter data from OVERFLOW '73, Hansen and Meincke (1979) described eddylike features in the frontal area that had time scales between several days and several weeks, and had horizontal scales of the order of 50 km. On a more recent survey Meincke (1978) discusses details and implications of water mass distributions around the Faeroe Islands. In particular, frontal features such as salinity minima were found to be advected southeastward at about 20 cm s^{-1}, north of the Faeroes.

A linearly enhanced infrared image from the TIROS-N polar orbiting satellite (Fig. 2) was provided by the University of Dundee, Scotland. The image was not geometrically corrected, but the Iceland–Faeroe Island front (IFF) was near the nadir point of the satellite and hence was minimally distorted (a distance scale is shown). Evidence of meanders, filaments, and eddylike features in the surface thermal front can be seen extending southeastward from Iceland. The scale of these features is approximately 50 km.

Findings—This paper discusses the analysis of CTD data from a survey made of the IFF by the U.S. Naval Oceanographic Office (NOO) in October 1980, in the region just north of the Faeroe Islands. An attempt is made to describe the many scales of variability of a portion of the front and to quantify some aspects of this variability. The results support earlier findings that there is significant alongfront dynamic variability on spatial scales of about 50 km and time scales as short as several weeks. Thermohaline features are highly variable, particularly in the upper 200 m. Interleaving of cold, Arctic water and warmer, Atlantic water occurs on vertical scales of the order of 50 m, consistent with those predicted by Ruddick and Turner (1979) for intrusions driven by double-diffusive convection. Calculations of heat flux (5.16×10^4 W m^{-2}) and salt flux

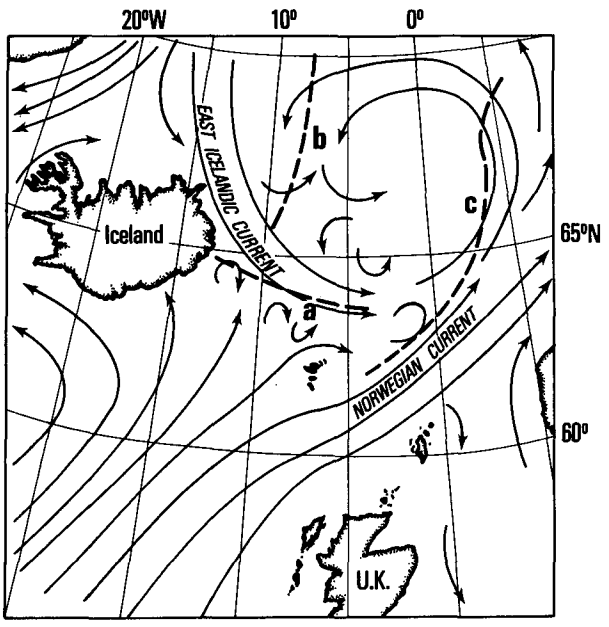

FIG. 1. Surface currents and frontal positions for the southern Norwegian Sea. (a) Iceland–Faeroe Island Front; (b) Jan Mayen Front; (c) Norwegian Current Front.

(1.58 g m^{-2} s^{-1}) across the front show larger values than those found in the Antarctic Polar Front by Joyce *et al.* (1978), but show values of the same order as eddy heat fluxes across the IFR found by Willebrand and Meincke (1980).

2. Observations

In October 1980, the NOO conducted a survey aboard USNS *Kane* near the Faeroe Islands in the southern Norwegian Sea. The survey constituted one part of a three-phase effort to describe upper ocean variability in the region, and its primary focus was the IFF north of the Faeroes. The bathymetry of the IFR and the locations of hydrographic stations are shown in Fig. 3. Cruise details are described by Hallock (1981), and a CTD data report was prepared by Teague (1981). CTD Stations 109–171 are discussed in this paper.

The majority of CTD stations were concentrated in rectangular grid straddling the IFF with an 18.5-km horizontal spacing (see Fig. 3). The first frontal section proceeded northeastward from Station 113 to Station 121. The following sections went alternately southwestward and northeastward. At most stations, a single CTD cast was made to within several meters of the bottom. At Station 117 a series of six 2.5-h "yo-yo" casts was conducted over a 36-h period. During each yo-yo cast the CTD was cycled continuously between about 50 and 250 m yielding a total of 21 down profiles separated by about 7 min. During the yo-yo cast discussed later in this paper the ship drifted 2.5 km in roughly a straight line, relative to the surface, in about

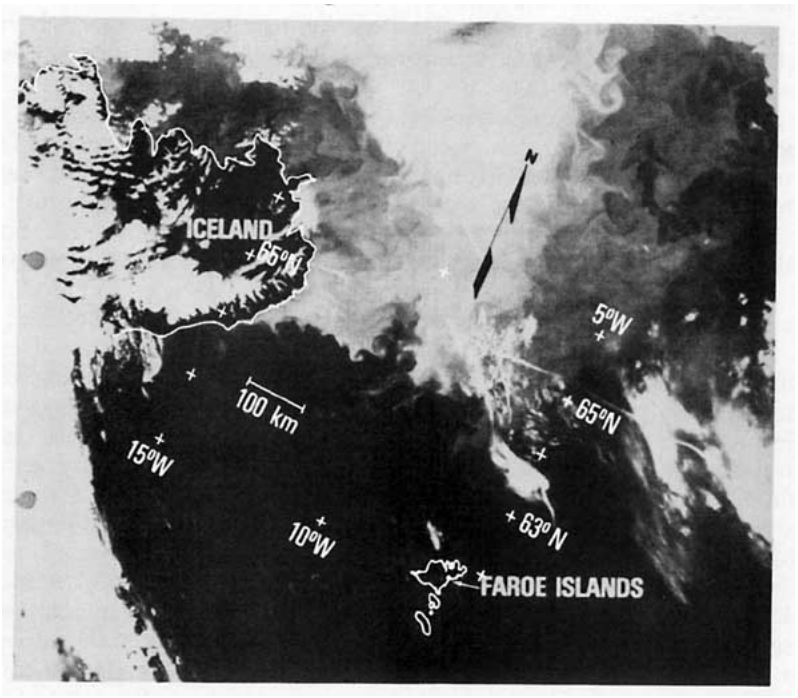

FIG. 2. Infrared image from the TIROS-N orbiting satellite, depicting the frontal region in the southern Norwegian Sea in spring 1980. The survey roughly straddled the surface front due north of the Faeroe Islands (Courtesy of the University of Dundee, U.K.).

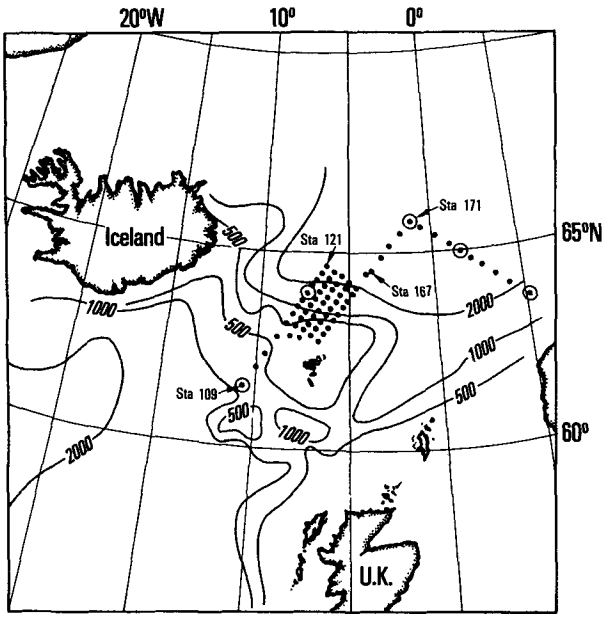

FIG. 3. Station locations. Circles indicate yo-yo stations. Bathymetry is in meters.

2.5 h, thus yielding a short section. Hence, the horizontal separation of individual downcasts was several hundred meters.

A series of AXBT flights over the region was carried out by NOO with their P-3 aircraft in 1979 and 1980. Hand analyses (contour maps) were prepared by NOO personnel during and after flights to provide a near real-time product. One set of flights took place during September and October 1980, just prior to and during the survey discussed in this paper. The flight most relevant to the frontal study occurred on 6 October and consisted of about 50 AXBTs dropped in the survey area. Analyses prepared from these data were available before the survey and were used to decide the exact location of the frontal grid of CTD stations. Contours of temperature at 100 m (Fig. 4) show a well-defined section of the front just north of the Faeroes, and the rectangle indicates the survey area. The 100-m data were selected since they represented the sharpest delineation of the front in the mixing layer.

3. Analysis and discussion

a. Large-scale characteristics

To provide a larger scale context for the frontal study a composite section was prepared that extends from Station 109 to Station 171. The frontal sections can be viewed as an x–y grid of 45 stations with the origin at Station 113 and with Stations 113–121 lying along the y-axis. Temperature, salinity, and σ_t were averaged on level surfaces over the five stations along x at each of the nine y positions. This averaged section was combined with Stations 109–112 and Stations 167–171 yielding the plots of Figs. 5–7. Temperature and salinity distributions for the majority of the survey data are shown in Fig. 8. The important water masses are summarized in Table 1.

Below 100 m, isotherms (Fig. 5) slope upward on approach to the IFR from the south. Just north of the IFR they become more horizontal and form the relatively sharp thermocline near 100 m. North of the IFR the cold, dense water below 500 m is the Norwegian Sea Deep water (NS), which flows out of the Norwegian Sea through the Faeroe–Shetland Channel. It is intermittently forced over the IFR by atmospheric effects or by eddylike motions in alongfront flows (Hansen and Meincke, 1979). Between the surface and about 100 m is the mixing layer and the more diffuse surface front.

North of Station 117 a salinity minimum (34.8 ‰ $< S <$ 34.9 ‰) is evident (Fig. 6) near 300 m, consistent with the results of OVERFLOW '60 (Tait, 1967). The tongue of low salinity resembles those found by Meincke (1978) and contains primarily North Icelandic/Arctic Intermediate water (NI/AI). Evidence of East Icelandic water (EIW) is not present. The near-surface waters just north of the IFF resemble East Icelandic Current water (EIC) but have higher salinities suggestive of mixing with North Atlantic water (NA). The broad scatter of T–S points (Fig. 8) in the range: 4–8°C, 34.85–35.1‰ is due mainly to data from just north of the IFF near the surface.

In Fig. 7 σ_t shows a structure similar to that of temperature including a weak density front at the surface

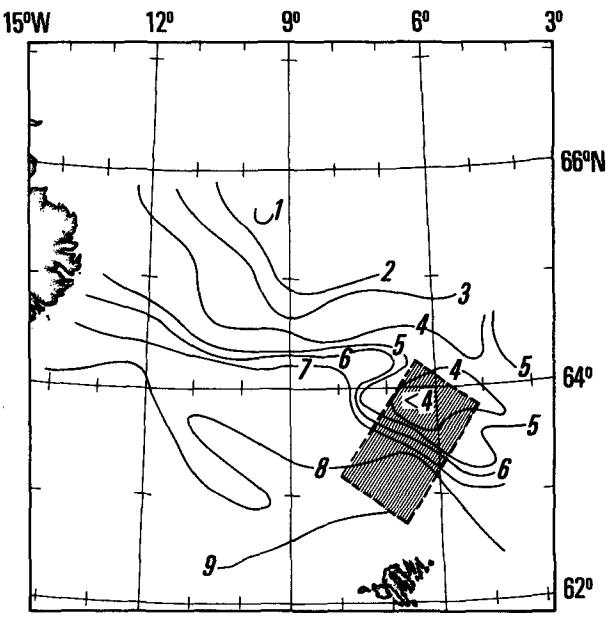

FIG. 4. Horizontal maps of AXBT temperature (°C) for 6 October 1980 at 100 m.

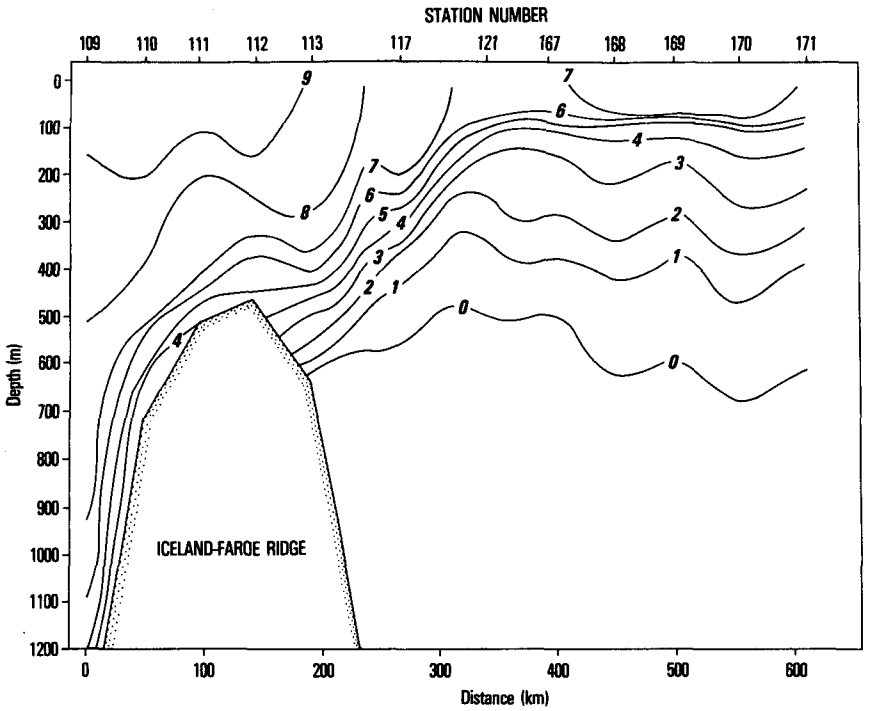

FIG. 5. Vertical section of temperature (°C) between Stations 109 and 171.

near Station 117. Differences in slopes of isopycnals and isotherms, as well as the form of the salinity field, indicate the presence of density-compensated variability or intrusive features.

b. Isopycnal variability of temperature and salinity

Significant dynamic variability is present in the vicinity of the IFF. Strong horizontal density gradients

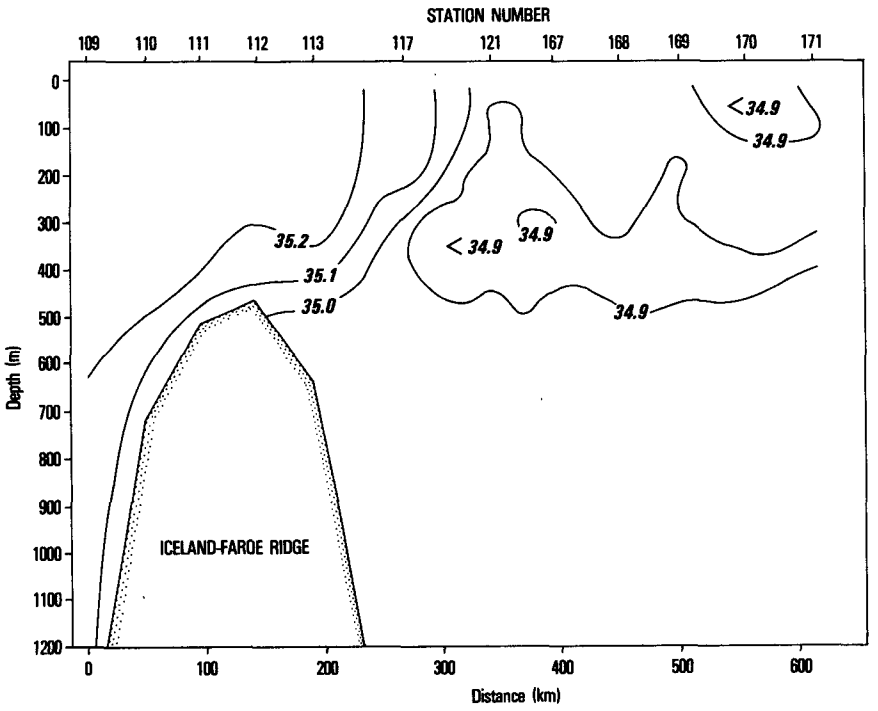

FIG. 6. As in Fig. 5 but for salinity (‰).

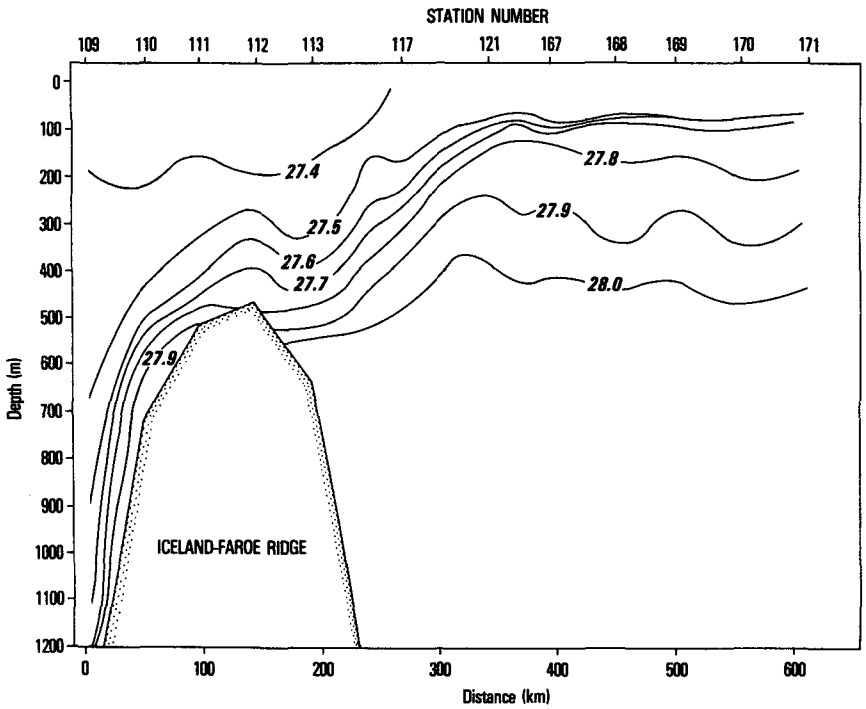

FIG. 7. As in Fig. 5 but for σ_t (kg m^{-3}).

imply geostrophic currents on larger scales and internal wave effects on shorter scales. Under such conditions, water mass boundaries and other thermohaline structures, such as intrusions, are somewhat obscured in sections of temperature and salinity alone. Introducing an enhanced representation of T–S variability to allow a better description of such features is useful. This is done by computing an average T–S relationship and temperature anomalies about this average, using σ_t as the independent variable. This isopycnal temperature anomaly (ITA) thus represents the density-compensated temperature change relative to the average T–S relation. To preserve the overall geometry in the presence of intense horizontal gradients of density, ITA may then be examined as a function of depth (rather than of σ_t).

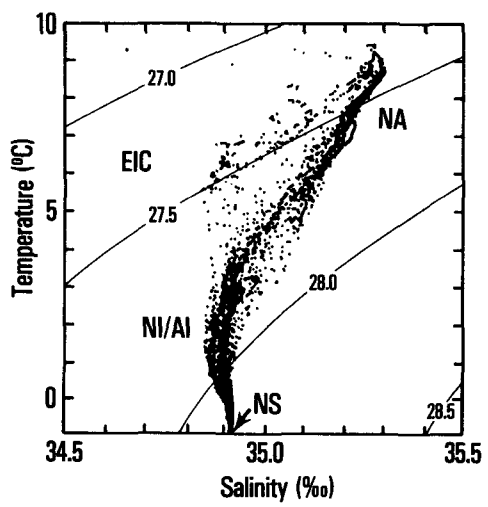

FIG. 8. Temperature–salinity scatter diagram for stations in the frontal grid (data are plotted every 10 m).

ITA provides a spatial perspective on T–S variability and a consistent means of defining an intrusion. A temperature inversion is almost always accompanied by a compensating inversion in salinity, and near a front, such inversions imply intrusive interleaving. However, inversions are not required for the existence of intrusive layers; only a layer of anomalous water (a layer of water whose T–S properties are isopycnically displaced relative to the norm for the region) is necessary. Hence weak intrusions, especially in the presence of dynamic features, are difficult to detect without careful examination of T–S diagrams. The ITA provides a systematic way to describe the geometry of intrusive features.

The ITA is roughly proportional to the quantity τ defined by Veronis (1972): a change in T and S is transformed into a change in σ_θ and τ, where the τ-axis is parallel to lines of constant σ_θ, while the σ_θ-coordinate is perpendicular. These coordinate axes lie in a normalized T–S plane and the choice of normalization is somewhat arbitrary. However, the ITA is a more natural quantity, since it is computed relative to an observation-based reference (the mean T–S curve), where τ anomalies are computed relative to an artificial reference curve.

TABLE 1. Water masses near the Iceland–Faeroe Ridge.

Water mass	Temperature (°C)	Salinity (‰)
North Atlantic water (NA)	$T > 9.0$	$S > 35.32$
Modified North Atlantic water (MNA)	$T > 8.5$	$S \approx 35.24$
East Icelandic Current water (EIC)	$6.0 < T < 6.5$	$34.45 < S < 34.65$
North Icelandic/Arctic Intermediate water (NI/AI)	$2.5 < T < 3.0$	$S \approx 34.88$
Norwegian Sea Deep water (NS)	$T < -0.5$	$S \approx 34.92$
East Icelandic Winter water (EIW)	$-0.5 < T < 1.0$	$S \approx 34.72$

Such an average T–S relation was calculated using most of the CTD data from the NOO survey. While the number of stations included in this calculation yielded a stable estimate, some finestructure remained. Consequently, the averages were smoothed prior to computing the anomalies. The resulting T–S curve together with an envelope of rms isopycnal anomalies of temperature and salinity are shown in Fig. 9. The geographical data distribution included in the average resulted in ITA = 0°C in the frontal zone just north if the IFR, as evident in the frontal sections described next.

c. *Frontal structure*

Each of the five frontal crossing sections (Fig. 2) was completed in about one day. There was a 36 h delay at Station 117 during the first section to conduct yo-yo CTD casts, so the entire frontal grid took about a week to complete. Dynamic height anomaly (DHA) of the surface relative to 500 db was computed for frontal grid data. A contour map of DHA (Fig. 10) reveals a cyclonic feature centered about 40 km north of the south edge of the grid, embedded in a predominantly eastward flow of about 20 cm s^{-1}. The implied current structure extends to 400 m with a maximum horizontal shear located about 20 km north of the center of the feature.

Temperature and ITA sections for the second and fifth frontal crossings (going from west to east) show pronounced differences in frontal structure (Figs. 11–14; the inset shows section position within the station grid). The first section (not shown) resembles the second, and the third and fourth (also not shown) resemble the fifth. The cyclonic fold is evident in the isotherms of Fig. 11. This feature does not appear in data obtained one month later in a repeat of the second section; it had decayed or, more likely, had propagated from the area in the intervening period. The horizontal and inferred temporal scales of the eddylike feature are about 50 km and several weeks, respectively, which is con-

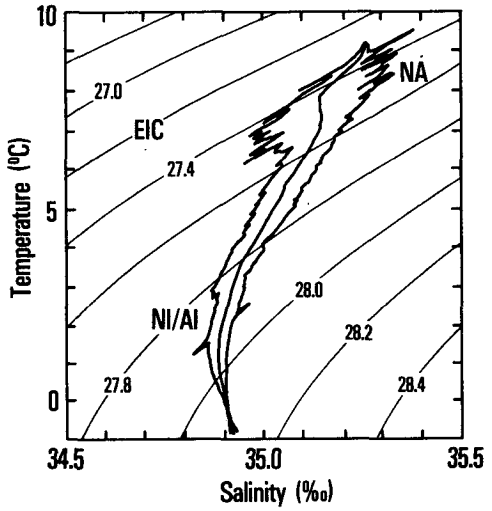

FIG. 9. Averate T–S curve with standard deviation envelope.

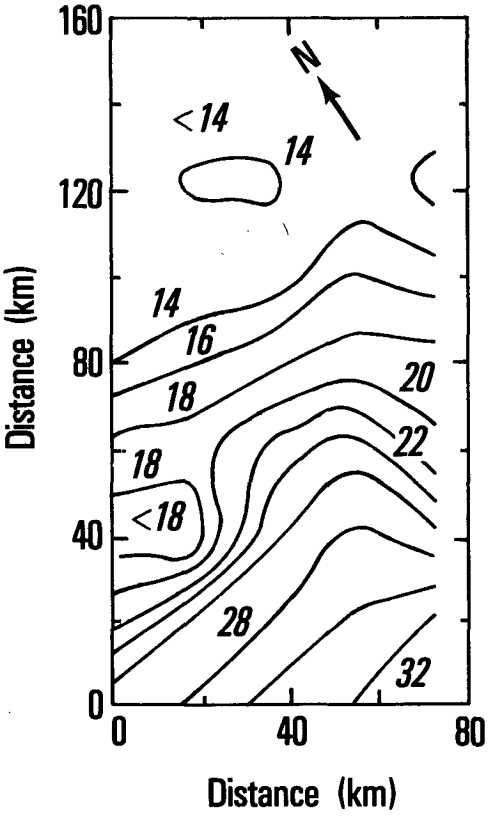

FIG. 10. Dynamic height anomaly (dyn cm) of the surface relative to 500 db in the frontal grid.

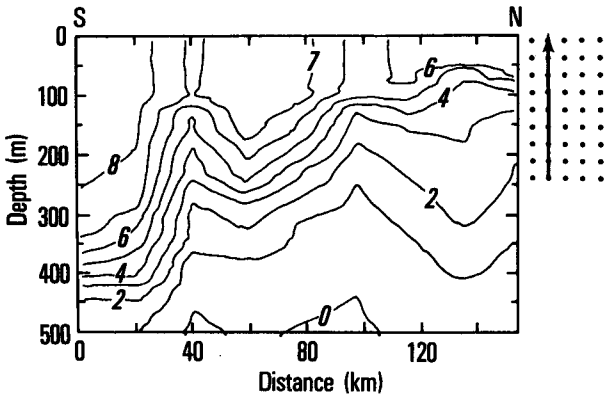

FIG. 11. Vertical section of temperature (°C) for frontal crossing 2 (inset shows position of section within frontal grid).

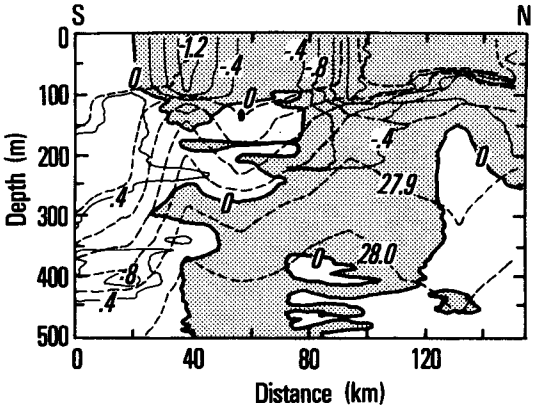

FIG. 13. Vertical section of isopycnal temperature anomaly (°C; solid) and σ_t (kg m^{-3}; dashed) for frontal crossing 2.

sistent with scales found by Hansen and Meincke (1979). The satellite image of Fig. 2 suggests that these frontal convolutions are ubiquitous in the area.

Inversions and small structures in the temperature field (not present in the density) imply intrusive interleaving that can be more clearly and quantitatively seen in sections of ITA (Figs. 13 and 14). Isopycnals have been included in the figures to show the relationship between ITA and density. The highly variable surface front dominates above 100 m. The position of the subsurface front is somewhat more stable and is roughly associated with the horizontal shear zone. An intrusive feature, delineated primarily by the contour of ITA = 0°C, appears near 200 m between 40 km and 80 km in sections 2 and 5. The vertical scale of the interleaving is of the order of 50 m. It is speculated that the presence of horizontal shear and the meandering of the alongfront flow might pinch off and isolate intrusive tongues to form globs of anomalous water. Such a process could enhance cross-frontal mixing processes. Several globs can be seen in the sections: e.g., (Fig. 14) near 300 m and 400 m between 60–80 km. Similar phenomena have been described in other regions by Toole (1982).

The synopticity of the frontal grid comes into question; while individual sections (except, perhaps, the first) are probably accurate, details of horizontal maps (e.g., Fig. 10) should be treated with caution. An unsuccessful attempt was made to synthesize a three-dimensional picture of the finescale features in the five cross-front sections. While the larger-scale frontal structure is coherent from section to section, the smaller-scale finestructure is not, implying that the sampling was inadequate for the details of the intrusions in the alongfront direction. This inadequacy may have been as much temporal as spatial.

d. Heat and salt flux calculations

Joyce (1977) proposed a model for estimating heat and salt flux across a front due to intrusive interleaving. In the model the vertical exchange of heat and salt across intrusion boundaries is balanced by horizontal advection along the layers. The model assumes equilibrium of the medium (interleaving) scale and also assumes isopycnal advection within the layers. The fluxes of temperature, salinity, and density are given by

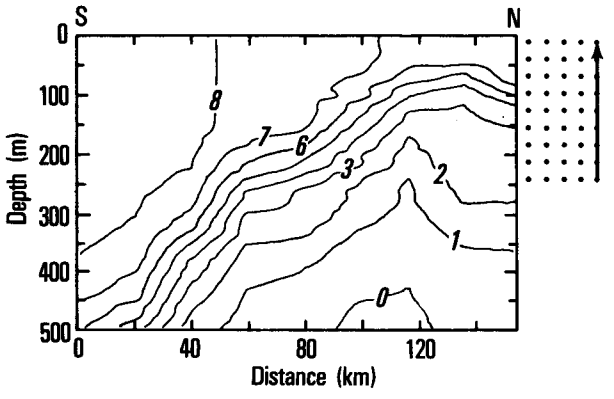

FIG. 12. As in Fig. 11 but for frontal crossing 5.

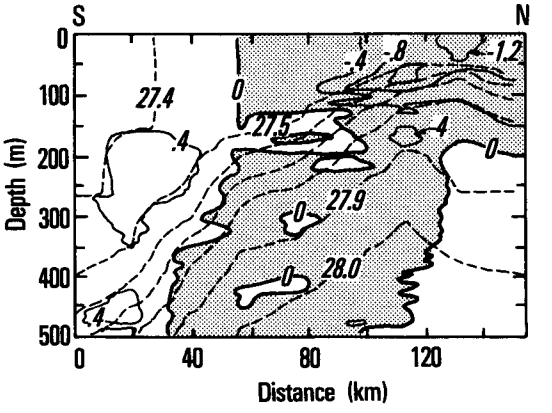

FIG. 14. As in Fig. 13 but for frontal crossing 5.

$$F_T = A_T{}^V \frac{\langle (\partial \tilde{T}/\partial z)^2 \rangle}{\partial \bar{T}/\partial y} \quad (1)$$

$$F_S = A_S{}^V \frac{\langle (\partial \tilde{S}/\partial z)^2 \rangle}{\partial \bar{S}/\partial y} \quad (2)$$

$$F_\rho = \rho_0(\beta F_S - \alpha F_T) \quad (3)$$

where

$$\alpha = -\frac{1}{\rho_0}\frac{\partial \rho}{\partial T}; \quad \beta = \frac{1}{\rho_0}\frac{\partial \rho}{\partial S}$$

and $A_T{}^V$, $A_S{}^V$, are the vertical eddy diffusivities of heat and salt; $\tilde{T}$ and $\tilde{S}$ are the medium-scale fields, taken here to be isopycnal anomalies. The ensemble average, denoted by angle brackets, represent an average on isopycnal surfaces over all 45 frontal stations. The overbar denotes the large-scale field and $d\bar{T}/dy$, $d\bar{S}/dy$ are average, cross-frontal gradients along isopycnals.

While $A_T{}^V$ and $A_S{}^V$ are not explicitly known, a value of 1 cm^2 s^{-1} is used where interleaving is present, as by Joyce *et al.* (1978). Interleaving is most pronounced between the 27.5 and 27.9 isopycnals, and $d\bar{T}/dy$ ranges from about 0.7×10^{-7} °C cm^{-1} to 1.7×10^{-7}°C cm^{-1}. A plot of F_T versus σ_t (Fig. 15) shows two relative maxima near σ_t = 27.6 and 27.75. The error bar reflects the uncertainty in $d\bar{T}/dy$.

The F_S displays a similar structure as a function of density but has only one pronounced maximum at σ_t = 27.6. Density flux computations using Eq. (3) show $F_\rho \approx 0$ near σ_t = 27.6 but a magnitude up to 65% of the average of $\alpha\rho_0 F_T$ and $\beta\rho_0 F_S{}^V$, near σ_t = 27.8. Ideally F_ρ should be 0 since the temperature and salinity fluxes are defined to be on isopycnal surfaces in the model. Actual values of F_ρ range from -1×10^{-4} g cm^{-2} s^{-1} to 2.7×10^{-5} g cm^{-2} s^{-1}, with an absolute minimum of -2×10^{-6} g cm^{-2} s^{-1} near σ_t = 27.62. The primary sources for the imbalances are probably the estimates of $d\bar{T}/dy$ and $d\bar{S}/dy$, as the error bar in Fig. 15 suggests.

To provide more stable estimates for comparison purposes vertical averages were calculated for temperature and salinity fluxes, and an average density flux formed from these:

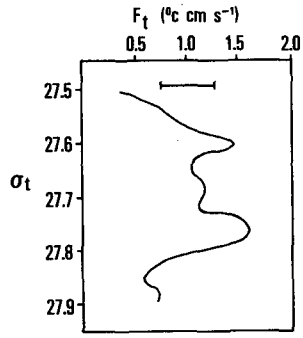

FIG. 15. Temperature flux (°C cm s^{-1}) for the frontal grid. The error bar reflects uncertainty in $\partial\bar{T}/\partial Y$.

$$F_T = 1.20 \pm 0.24\text{°C cm s}^{-1}$$

$$F_S = 0.154 \pm 0.041 \text{ ‰ cm s}^{-1}$$

$$F_\rho = (-2.3 \pm 4.5) \times 10^{-5} \text{ g cm}^{-2} \text{ s}^{-1}$$

with $\alpha = 0.12 \times 10^{-3}$ (°C)$^{-1}$ and $\beta = 0.79 \times 10^{-3}$ (‰)$^{-1}$. These fluxes are significantly higher than those found by Joyce *et al.* (1978) for the Antarctic Polar Front. The differences are due to both a greater implied vertical flux and weaker, mean cross-front gradients in the IFF. The F_T may be expressed as a heat flux (power per unit area):

$$F_H = \rho_0 C_P F_T = 5.16 \times 10^4 \text{ W m}^{-2}$$

where C_P is the specific heat of water [1 cal g^{-1} (°C)$^{-1}$] and F_{salt} as salt flux [$10\ \rho_0 F_S = 1.58$ g (salt) m^{-2} s^{-1}]. The eddy heat flux was calculated across the IFR from current meter and temperature records from 17 m above the bottom (534 m) (Willebrand and Meincke, 1980). They found $\rho_0 C_P \langle U'T' \rangle = 1.2 \times 10^5$ W m^{-2}, about 2.5 times higher than the value of F_H above. The eddy heat flux (and hence F_H) was concluded to be locally comparable to advection by the East Icelandic Current and by the overflow of NS over the IFR, but was small compared to the total heat budget of the Norwegian Sea.

e. *Salt finger effects*

The case for interleaving driven by double-diffusion has been dealt with by Stern (1967), Ruddick and Turner (1979), Toole and Georgi (1981) and Garrett (1982). If intrusions are driven by double-diffusive convection (salt fingers), then the downward density flux due to salt flux ($F_S{}^V$) would be about twice that due to heat flux ($F_T{}^V$), resulting in a net downward density flux—i.e., the salt fingers transport salt downward more efficiently than heat. The ratio of these fluxes for oceanic conditions (suggested by Ruddick and Turner) is $F_T{}^V/F_S{}^V \approx 0.56 = n$ implying that cool, fresh intrusions become more dense relative to the ambient water while warm, salty intrusions become less dense. A simple argument was proposed relating the vertical interleaving scale to the larger-scale vertical and horizontal property gradients. The argument places an upper and lower bound on layer thickness. An initial state of a purely thermohaline front (i.e., no horizontal density gradient) separating two regimes was assumed. The vertical density gradient is controlled in one regime by temperature and in the other by salinity. An intrusion pair (warm salty over cool fresh) is hypothesized to occur across the front, and salt finger convection is assumed to proceed until both layers have the same salinity. An upper bound on layer thickness is set by requiring that the potential energy of the water column either decreases or remains constant during the process. A lower bound on layer thickness is set by preventing

the occurrence of density inversions as a result of the mixing. A combined statement of these criteria is:

$$H = \frac{\frac{3}{2}(1 - n)\beta\Delta\bar{S}}{(1/\rho_0)\partial\rho/\partial z}$$

where

H layer thickness (within a factor of two),
n density flux ratio (defined above = 0.56),
$\Delta\bar{S}$ cross-frontal isopycnal salinity change,
$\partial\rho/\partial z$ vertical density gradient.
$\Delta\bar{S}$ = 0.2 ‰ from the previous section, and from Fig. 7

$$\frac{1}{\rho_0}\frac{\partial\rho}{\partial z} = (1, 2, 4) \times 10^{-6}\ \mathrm{m}^{-1},$$

where a range is given for the density gradient in the frontal zone. The resulting vertical scale H = (25, 50, 100) m is the primary vertical scale observed in the various data presentations.

A closer examination of the intrusion scales is possible with data from the yo-yo series at Station 117. The ITA and σ_t for a yo-yo cast near Station 117 are shown in Fig. 16. There are about 20 downgoing profiles in the section, which is oriented roughly across-front. Relatively warm, saline tongues slope upward across isopycnals, while the interleaving cool tongues slope in the opposite sense. Shaded areas denote density ratio $\alpha\partial T/\partial z(\beta\partial S/\partial z)^{-1}$ less than 2, indicating conditions favorable for salt finger convection. The vertical extents of the tongues are within the range predicted by the foregoing argument. Taken together, these points suggest that the observed interleaving is consistent with a double-diffusive driving mechanism. Furthermore, the vertical salt fluxes implied might be used to modify the model previously discussed.

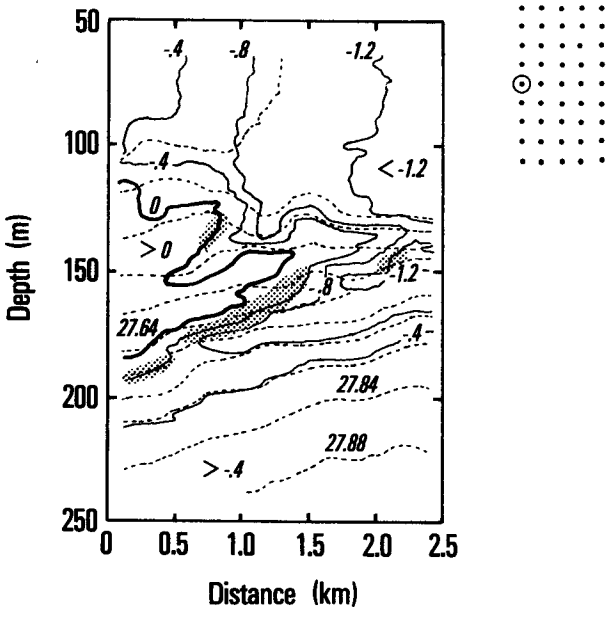

FIG. 16. Isopycnal temperature anomaly (°C; solid) and σ_t (dashed) for a yo-yo section at Station 117. Shaded areas indicate conditions favorable for salt fingering (inset shows position of Station 117 within the frontal grid).

4. Summary and conclusions

With a telescoping perspective, a section of the oceanic polar front near the Iceland–Faeroe Ridge has been described. The front results from the confluence of different water masses and exhibits strong spatial and temporal variability.

The surface expression of the front, to a depth of about 100 m, is convoluted by eddylike features probably along its entire length. It is a wide (70 km) swath populated by many folds and segments of more intense frontal gradients. The subsurface front, from about 100 m to the depth of the IFR, is a better defined feature and appears to be less convoluted than the surface signature. It slopes significantly from the vertical (southward from the northern edge) and shows strong evidence of intrusive interleaving that may well be driven by double-diffusive convection. While transports of properties across the front by intrusive mixing alone appear insignificant in comparison to overall balances of the Norwegian Sea, they are locally important and are of the same order as eddy transports. The latter are evidenced by the presence of anomalous globs found on both sides of the front.

In conclusion, alongfront structure and temporal variability present difficulties for two-dimensional frontal models. Obviously some aspect of along-front variability, which includes propagating mesoscale features, must be included in realistic simulations. The structure and evolution of such features must be better understood observationally, however, before effective modeling is possible.

Recommendations for a future frontal survey are as follows:

- Include intense alongfront hydrographic sampling to describe convolutions better. Using a current profiler is suggested. Synopticity is a primary concern here.
- Study the evolution of globs of anomalous water. Where do they go? How long do they persist? The ability to do on-board, near-real-time data analysis would be required, and efficient, precise navigation is a must.
- Deploy current meter moorings at selected locations along the IFR with instruments as near to the surface as practicable. Using inverted echo sounders would provide a means to monitor the position of the thermal front at selected points.
- Additional yo-yo or chain observations might provide better statistics on interleaving scales. Using a Doppler acoustic current profiler (ship-mounted) would provide necessary relative velocity information during CTD casts or chain tows.

• Concurrent satellite coverage would provide needed perspective on the survey. In particular, the availability of satellite altimeter data would provide a direct measure of the mesoscale fields and would not be severely affected by the frequent cloud cover in the region.

Acknowledgments. I would like to thank Drs. A. W. Green and R. Hollman for their comments. This work was supported by the ASW Oceanography Program under program element 63704N.

REFERENCES

Dooley, H. D., and J. Meincke, 1981: Circulation of water masses in the Faeroes channels during OVERFLOW 73. *Dtsch. Hydrogr. Z.*, **34**(2), 41–55.

Garrett, C., 1982: On the parameterization of diapycnal fluxes due to double-diffusive intrusions. *J. Phys. Oceanogr.*, **12**, 952–959.

Hallock, Z. R., 1981: Report of Operations, USNS *Kane:* Northeast Atlantic and Norwegian Sea survey operation 270980 phases I, II, III, 16 September–28 November 1980. U.S. Naval Oceanographic Office, OCS-270980, 51 pp.

Hansen B., and J. Meincke, 1979: Eddies and meanders in the Iceland–Faeroe Ridge area. *Deep Sea Res.*, **26A**, 1067–1082.

Helland-Hansen, B., and F. Nansen, 1909: The Norwegian Sea. *Rep. Norweg. Fish. Mar. Invest.*, **2**, 390 pp.

Joyce, T. M., 1977: On the lateral mixing of water masses. *J. Phys. Oceanogr.*, **7**, 626–629.

——, W. Zenk and J. M. Toole, 1978: The anatomy of the Antarctic Polar Front in the Drake Passage. *J. Geophys. Res.*, **83**(C12), 6093–6113.

Meincke, J., 1978: On the distribution of low salinity waters around the Faeroes. *Dtsche. Hydrogr. Z.*, **31**(2), 50–64.

Mueller, T. J., J. Meincke and G. A. Becker, 1979: The distribution of water masses on the Greenland–Scotland Ridge in August–September, 1973. *Ber. Inst. Meeresk.*, **62**, 1–172.

Ruddick, B. R., and J. S. Turner, 1979: The vertical scale of double-diffusive intrusions. *Deep Sea Res.*, **26A**, 903–913.

Stern, M. E., 1967: Lateral mixing of water masses. *Deep Sea Res.*, **14**, 747–753.

Tait, J. B., Ed., 1967: The Iceland–Faeroe Ridge International (ICES) Overflow Expedition, May–June 1960. *Rapp. P.-V. Réun., Cons. Intl. Explor. Mer*, **157**, 1–274.

Teague, W. J., 1981: CTD profiles in the Northeast Atlantic and Norwegian Sea: September–November, 1980. Data Summary, U.S. Naval Oceanographic Office, NSTL, Mississippi.

Toole, J. M., 1982: Intrusion characteristics in the Antarctic Polar Front. *J. Phys. Oceanogr.*, **22**, 780–793.

——, and D. T. Georgi, 1981: On the dynamics and effects of double-diffusively driven intrusions. *Progress in Oceanography,* Vol. 10, Pergamon, 123–145.

Veronis, G., 1972: On properties of seawater defined by temperature, salinity, and pressure. *J. Mar. Res.*, **30**(2), 227–255.

Willebrand, J., and J. Meincke, 1980: Statistical analysis of fluctuations in the Iceland-Scotland frontal zone. *Deep Sea Res.*, **27A**, 1047–1066.